EUKARYOTIC CELL, June 2009, p. 852–857 Vol. 8, No. 6
1535-9778/09/$08.00+0 doi:10.1128/EC.00379-08

Formation of Hirano Bodies after Inducible Expression of a Modified Form of an Actin-Cross-Linking Protein▽

Juan F. Reyes,† Karen Stone, Jeanie Ramos,‡ and Andrew Maselli*

Chicago State University, Department of Biological Sciences, 9501 S. King Drive, Chicago, Illinois 60628

Received 1 December 2008/Accepted 26 March 2009

Hirano bodies are cytoplasmic inclusions composed mainly of actin and actin-associated proteins. The formation of Hirano bodies during various neurodegenerative disorders, including Alzheimer's disease and amyotrophic lateral sclerosis, has been reported. Although the underlying molecular mechanisms that lead to the formation of these inclusions in the brain are not known, expression of the C-terminal fragment (CT) (amino acids 124 to 295) from the endogenous 34-kDa actin-binding protein of *Dictyostelium discoideum* leads to the formation of actin inclusions in vivo. In the current study, we report the development of an inducible expression system to study the early phases of Hirano body formation using an inducible promoter system (*rnrB*). By fusing the CT to a green fluorescent protein (CT-GFP), we monitored protein expression and localization by fluorescence microscopy, flow cytometry, and Western blot analysis. We observed an increase in the number and size of inclusions formed following induction of the CT-GFP vector system. Time-lapse microscopy studies revealed that the CT-GFP foci associated with the cell cortex and fused to form a single large aggregate. Transmission electron microscopy further demonstrates that these inclusions have a highly ordered ultrastructure, a pathological hallmark of Hirano bodies observed in postmortem brain samples from patients with various neurodegenerative disorders. Collectively, this system provides a method to visualize and characterize the events that surround early actin inclusion formation in a eukaryotic model.

Neurodegenerative diseases are characterized pathologically by the formation of protein deposits localized to specific regions of the brain. Notably, protein aggregates derived from the amyloid precursor protein, the microtubule-associated protein tau, and α-synuclein have received much attention. However, the intracellular aggregations of actin and actin-binding proteins known as Hirano bodies are less well known. Hirano bodies were first identified in brains affected by Pick's disease and amyotrophic lateral sclerosis (8, 17). Subsequent studies identified these aggregates in a number of neurodegenerative diseases and other conditions that cause persistent brain injury (7). Although it is clear from this and other observations that the main constituents of Hirano bodies are actin and actin-binding proteins which assemble to form a characteristic ultrastructure (3), little is known about the mechanisms that underlie Hirano body formation. To further understand the spatial and temporal events that surround the formation of these inclusions in vivo, a live cell model that mimics the formation of these structures is necessary. The discovery that *Dictyostelium discoideum* cells expressing a carboxy-terminal fragment (CT) of the 34-kDa calcium-sensitive actin-binding protein (ABP34) form Hirano bodies in vivo (1, 12, 13) provides a tantalizing clue to a possible mechanism of protein aggregation.

Using *Dictyostelium* as a live cell model system provides the opportunity to control protein expression levels. In this study, we report the expression of the CT fused to green fluorescent protein (GFP) under the control of a constitutive (actin 15) and an inducible ribonucleotide reductase (*rnrB*) promoter using the DXA-GFP2 and RNR plasmid vectors, respectively (4, 10, 11). Using this system, we demonstrate that a fusion between the CT and the GFP tag (CT-GFP) provides a unique stable probe to observe CT dynamics in living cells. Expression of the CT-GFP fusion from the inducible RNR system triggered the formation of small protein inclusions visible by fluorescence microscopy at basal expression levels. Following promoter induction, there was a robust increase in the size and number of protein aggregates formed. Over time, the number of total inclusions decreased, but the average size of the remaining aggregates was larger. Our observations of live cells expressing CT-GFP show a pattern of aggregate formation where small aggregates combined to form larger inclusions. These inclusions were usually found at the rear of moving *Dictyostelium* cells.

MATERIALS AND METHODS

Cells and growth conditions. *Dictyostelium discoideum* wild-type (AX2) cells and transformed cell lines were grown in HL-5 medium at 20°C in 100-mm tissue culture plates as previously reported (2).

Plasmid construction. The CT-coding sequence (amino acids 124 to 295) was amplified from the p34kDa-myc plasmid (13) using primers 5′-CCG AAG CTT ATG TCT CAA CCA CAA ATG-3′ (5′) and 5′-ATG CCA GGT GTT TTC TTT CCA TGG CGG-3′ (3′) containing HindIII and KpnI restriction enzyme sites, respectively. The PCR product was ligated into pDXA-GFP2 (10), forming the CT-GFP fusion construct under the control of a constitutive promoter. The CT-GFP-coding sequence was amplified from pDXA-CT-GFP using primers 5′-CGC CGG AGA TCT GGT ACC AGT AAA GG-3′ (5′) and 5′-AAC ACC AAC TCT CTA GTA TCT AGA CGG-3′ (3′) containing BglII and XhoI restriction sites. The resulting PCR product was ligated into pRNR-P (4), assembling the pRNR-CT-GFP fusion construct under the control of an inducible promoter system. The pRNR-CT was built by amplifying the CT sequence using 5′-CGC CGG AGA TCT GGT ACC AGT AAA GG-3′ and 5′-3′CTT CTT CTA

* Corresponding author. Mailing address: Department of Biological Sciences SCI-310, 9501 S. King Drive, Chicago IL 60628. Phone: (773) 995-3298. Fax: (773) 995-3759. E-mail: amaselli@csu.edu.

† Present address: The Feinberg School of Medicine, Northwestern University, Chicago, IL.

‡ Present address: University of California, Santa Cruz, CA.

▽ Published ahead of print on 10 April 2009.

GAG TTG ATT ACG CGT CCG GCC-3′ containing BglII and XhoI restriction sites. The resulting PCR product was ligated into pRNR-P (4). All plasmids were screened and selected using XL1-Blue *Escherichia coli* strains (Stratagene, La, Jolla, CA) or JM109 (Promega, Madison, WI) and standard molecular biology techniques (16).

Transformation of wild-type (AX2) *Dictyostelium discoideum* cells by electroporation. Wild-type *Dictyostelium* cells were washed twice in ice-cold H-50 buffer as previously reported (5) and resuspended to 5.0×10^7 cells per ml in H-50. For each transformation, 100 μl of cells were added to a sterile, ice-cold, 0.1-cm electroporation cuvette. Following the addition of 4 μg of DNA, cuvettes were pulsed twice at 0.85 kV with a capacitance of 25 μF using a Gene Pulser XCell electroporator (Bio-Rad, Hercules, CA), as described by Gaudet et al. (5). After electroporation, cells were transferred to HL-5-containing plates and grown overnight. Cells were then selected with G418 antibiotic (10 μg/ml) at 24 h postelectroporation and cloned by limiting dilution in 96-well plates. Clones expressing pDXA-CT-GFP were selected for expression of GFP signal. Clones expressing pRNR-CT-GFP were split into replicate plates and screened for lowest basal levels of protein expression and highest induction levels as observed by large bright inclusions. Cell cultures were not maintained in culture for more than 30 days; new cultures were started from dimethyl sulfoxide stocks kept at −80°C. This procedure helped to avoid phenotypic drift, which was observed in cell lines as a reduction of the number of cells that are able to produce a visible GFP bright inclusion.

RNR promoter induction, the UV induction method. To determine the optimal RNR promoter induction conditions, transformed cells were grown axenically in HL-5 medium to mid-log phase in 100-mm culture plates before induction (Corning Co.). Cells were collected and centrifuged using an accuSpin 3R (Fisher Scientific) at 400 × *g* and washed once in MCPB buffer (10 mM Na_2HPO_4, 10 mM KH_2PO_4, 2 mM $MgCl_2$, 0.2 mM $CaCl_2$, pH 6.5). Cells were replated in 10 ml MCPB for 15 min in plates to allow the cells to adhere. Cells were then exposed at different UV energy levels (150, 250, and 500 J per m^2) with the lid off to expose cells directly to light using a CL-1000 UV light cross-linker (UV-Products). Immediately after exposure, MCPB was removed and replaced with HL-5 medium without disturbing cell adhesion. Other induction systems were tested, including the chemical DNA-damaging agents methylmethane sulfonic acid and 4-nitroquinoline 1-oxide. The chemical DNA-damaging agents were substantially more difficult to use and resulted in inconsistent results; therefore, only results of the UV light induction method are reported.

Image collection. Images for Hirano body size analysis were collected using a Zeiss Axiovert 25 equipped with a Q Imaging digital camera (Retiga 1300i) and a Windows computer running Image Pro Plus. Cell images were taken using a 32× objective and either LabTek chamber slides with a coverglass bottom or Corning six-well cluster plates (Nalge Nunc International,). Images of fixed cells were taken with a 40×, 63×, or 100× objective. An exposure time was selected to maximize the Hirano body observation and minimize background signal. In order to avoid investigator bias in experiments involving selecting clusters of cells expressing GFP, a mask of household self-adhesive shelf liner with holes punched at random using a standard paper punch was placed on the bottoms of six-well plates, creating random sample windows. After cell induction, TIFF images of areas visible through the mask were collected.

Phalloidin staining. Cells were allowed to adhere to glass microscope slides for at least 30 min in MCPB. Attached cells were then fixed in MCPB containing 1% paraformaldehyde, 0.1% glutaraldehyde, and 0.1% Triton X-100. Cells were then incubated in MCBP with 1% bovine serum albumin (BSA) for 15 min. The MCBP-BSA was then replaced with MCPB-BSA containing 1:500 rhodamine phalloidin (stock concentration of 100 mg/ml in methanol). Cells were washed, mounted, and then observed with a Zeiss Axio Observer equipped with an mRM camera and Axio Vision software.

Time-lapse series. Cells were placed at a concentration of 10^5 cells per chamber in a Lab-Tek no. 1.0 Borosilicate coverglass chamber slide (Nalge Nunc International). Cells were allowed to adhere to the coverglass for 15 min in HL-5 medium. Time-lapse images were then collected every 60 s using a Zeiss Axio Observer and mRM camera. To reduce UV exposure, the shortest exposure time with the lowest illumination level was chosen.

Size and distribution of Hirano bodies within the population. Images were collected as described above and analyzed using the public domain NIH Image program (developed at the National Institutes of Health and available on the Internet at http://rsb.info.nih.gov/nih-image/). A threshold level was selected to highlight pixels that represented the GFP signal, and images at different time intervals postinduction (0, 3, 6, 9, and 24 h) were analyzed. The automated counting function on the threshold image along with the area function was used to measure the brightness of GFP inclusions. The numerical data were exported to Microsoft Excel. Inclusions with an area of less than 5 pixels were not included in the analysis due to the background signal within the system. Pixel measurements were converted to μm^2 by using an image of a stage micrometer. The percentage of cells in the population with Hirano bodies was calculated by counting the number of cells with Hirano bodies above 5 pixels in the TIFF images collected and dividing by the total number of cells at 24 h after UV induction.

EM. The *Dictyostelium* cell lines described above were prepared for electron microscopy (EM) as described by Novak et al. (14). Briefly, aliquots containing 2.0×10^7 cells were harvested directly from plate culture in HL-5 medium and added to an equal volume of HL-5 containing 6% glutaraldehyde. The cells were pelleted after 3 to 5 min of incubation and resuspended in 5 ml of 3% glutaraldehyde, 0.2% tannic acid in 20 mM MOPS (morpholinepropanesulfonic acid), 5 mM EGTA, 5 mM NaN_3 and 5 mM $MgCl_2$ at pH 6.8. All washes were done by resuspension of cells and immediate centrifugation. The cells were postfixed in 1% OsO_4 for 20 min and washed before en bloc staining in aqueous 2% uranyl acetate on ice for 30 min. The samples were then washed again in ice-cold water as described above, dehydrated through a graded series of ethanol solutions, and embedded in Epon epoxy resin (Embed 812; Electron Microscopy Sciences, Hatfield, PA) in microcentrifuge tubes. Only a portion of the cells were embedded as small pellets to permit complete infiltration. Wild-type, induced, and noninduced cells were then analyzed for Hirano body inclusions at different times postinduction. Sections were viewed on a transmission electron microscope (1200 EX; JEOL, Tokyo, Japan), and negatives were scanned (Epson Perfection 4990 Photo) and prepared for presentation in Adobe Photoshop (San Jose, CA).

FACS analysis. Cells were induced at 250 J/m^2 as described above. After induction, cells were harvested at selected time points (0, 1, 3, 6, 9, and 24 h) after promoter induction and then centrifuged at 500 × *g*. The supernatant was removed, and a total volume of 2 ml ice-cold Sorensen's buffer was added to samples followed by 6 ml of cold 70% ethanol while vortexing. Samples were held in ice no longer than 24 h before analysis. Immediately before analysis, the samples were centrifuged to remove the ethanol. The pellet was resuspended in 2 to 3 ml Sorensen's buffer at 1×10^6 cells/ml. Fluorescence-activated cell sorter (FACS) analysis was performed on a BD-FACSAria (BD-Biosciences, San Jose, CA) using 488-nm excitation and 519-nm emission filters. The data presented represent the data from 10,000 events collected by the BD-DIVA software. The error bars represent the standard error of the mean. The experiment was repeated four times with consistent results; results from a representative experiment are presented.

RESULTS

Formation of CT-GFP inclusions. Fluorescent protein tags have provided invaluable information regarding protein-protein interactions and protein localization in different cellular systems. In this study, we describe the changes in the actin cytoskeleton that result from expression of a truncated actin-binding protein (CT) using fluorescence microscopy and transmission EM (TEM). To verify that our C-terminal fusion between the CT and the GFP tag produced a protein expression product capable of initiating protein aggregate formation, a constitutive CT-GFP vector was constructed using the pDXA system. When the pDXA-CT-GFP was introduced into *Dictyostelium* (AX2) cells, inclusions were clearly visible by fluorescence microscopy at 8 h postelectroporation. Expression of a fusion protein (CT-GFP) was further confirmed by Western blot analysis using an antibody against GFP (data not shown). Following selection with antibiotic, the majority of the population showed GFP-labeled inclusions. Representative cells expressing CT-GFP illustrating colocalization between GFP and F-actin by rhodamine phalloidin staining are shown in Fig. 1, row A. Similarly, cells expressing CT without the GFP tag formed inclusions visible by rhodamine phalloidin staining (data not shown). Wild-type cells lacking CT expression did not show any notable inclusions (Fig. 1, row D). We observed a more uniform presence of inclusions in populations expressing the pDXA-CT-GFP system then in populations expressing the pCT-myc system previously reported (12).

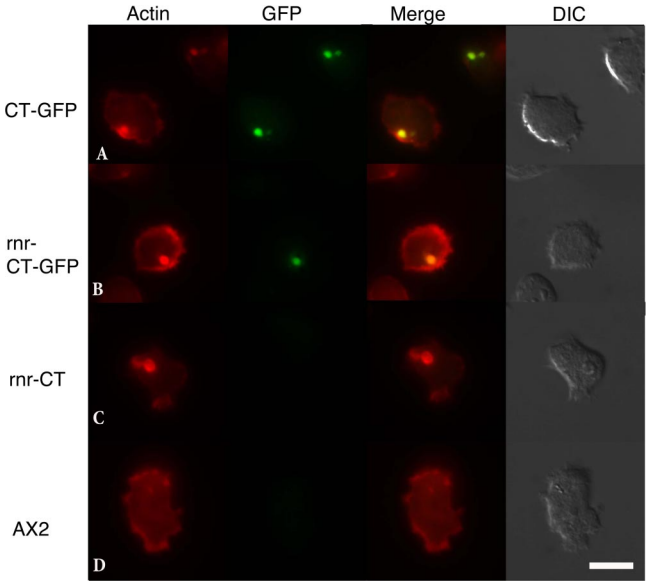

FIG. 1. Rhodamine phalloidin-stained cells. Row A, DXA-CT-GFP cells continuously produce large amounts of CT-GFP protein and form Hirano bodies. Row B, cells containing the pRNR-CT-GFP sequence show inclusions, which colocalize with F-actin and GFP. Row C, cell lines expressing the CT sequence alone from the RNR promoter show inclusions visible after phalloidin staining. UV light exposure did not have a discernible effect on AX2 cells. All cell lines, including AX2 (row D) wild-type populations, show the presence of F-actin in the cell cortex and other regions of dynamic actin activity. (Scale bar, 10 μm.) Images were taken at 24 h after promoter induction.

CT-GFP inducible promoter expression. The p-RNR plasmid contains a promoter inducible by DNA damage, which provides a positive regulation system. The promoter is composed of a 450-bp gene sequence (*rnrB*) encoding the RNR catalytic subunit, which senses a DNA damage event and induces promoter expression (4). Cells transformed with the RNR-CT-GFP vector were selected with antibiotic (G418). Twenty-four hours after UV induction, cells were fixed and stained with rhodamine phalloidin. Extensive colocalization was observed between GFP and the F-actin filaments throughout the actin aggregates formed (Fig. 1, rows A and B). Similar inclusions were observed in cells expressing the CT fragment alone but were not GFP positive (Fig. 1, row C). In cell lines expressing the RNR-GFP vector alone, no visible GFP fluorescence or actin inclusions were observed, a result consistent with those obtained by Gaudet et al. (4) (data not shown). Actin aggregates produced using the inducible RNR system appeared similar in shape and ultrastructure to actin aggregates formed using the constitutive actin promoter (Fig. 1 and 2) and to actin inclusions previously reported (12). These results further confirm the formation of actin inclusions following CT expression using different expression systems.

In our previous work, we showed that expression of the CT lacking GFP in *Dictyostelium* (12, 13) forms actin structures with similar characteristics in shape and ultrastructure as Hirano bodies from human brain biopsy samples (8, 17). To verify that cells expressing the CT-GFP fusion were capable of forming inclusions with similar ultrastructure, cells were fixed

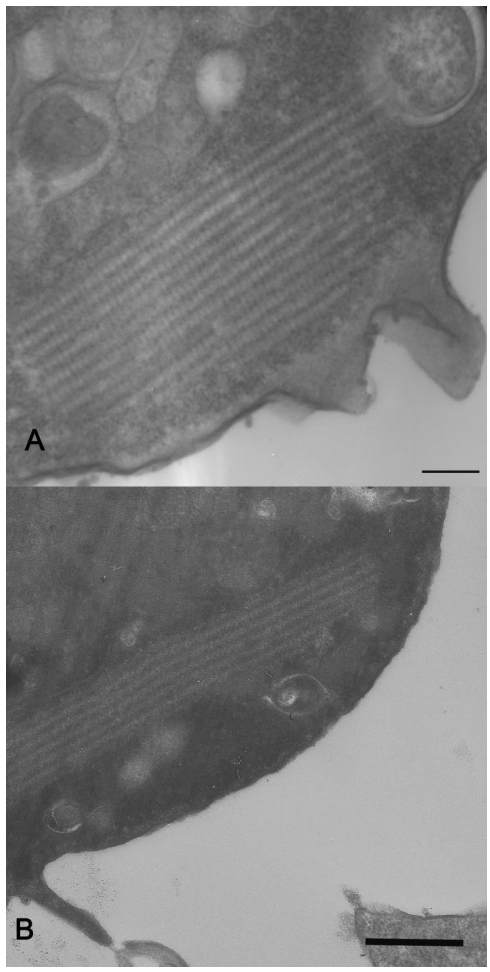

FIG. 2. TEM of AX2 cells expressing CT-GFP. (A) Cell expressing CT-GFP from a constitutively active promoter. (B) RNR-CT-GFP cells at 24 h after UV exposure. Note the highly ordered structures present in the cytoplasm of both types of cells. Scale bar, 200 nm.

and analyzed by TEM. Cells expressing the constitutive or inducible CT-GFP construct contained highly ordered regions that are characteristic of Hirano bodies (Fig. 2A and B). It is clear that the morphology of these structures ranges from regions of amorphous structure where all other organelles are excluded to regions where the laminar nature of classic Hirano bodies is clearly evident (Fig. 2). Characteristic highly ordered structures were not observed in wild-type cells or cells expressing full-length ABP34-GFP or GFP alone (data not shown). Actin aggregates produced using the inducible RNR system appeared similar in shape and ultrastructure to actin aggregates formed using the constitutive promoter and to actin inclusions previously reported (13).

Optimal induction conditions. The RNR system has been reported to have different basal expression levels within cells in a population. This may be due to the integration locus of plasmids or other processes that are still poorly understood (4).

To optimize our UV induction protocol, cloned cell populations were induced at increasing energy levels (0, 150, 250, 500, 3,000, and 10,000 J/m^2), and inclusions were measured at 24 h postinduction. A correlation was observed between the

levels of UV light used and the average number of actin inclusions formed. In cells exposed to 250 J/m^2, 64% of the cells contained Hirano bodies. Similarly, cells induced at 150 J/m^2 showed 56% of cells with inclusions. Unexposed populations showed inclusions in 37% of the cells, likely due to basal expression levels. Furthermore, we observed a positive relationship between the UV dosage and the inclusion size formed. For example, at 24 h after induction, populations exposed to 250 J/m^2 showed an average inclusion area of 1.5 μm^2, populations exposed to 150 J/m^2 showed an average area of 1.1 μm^2, and unexposed controls showed an average area of 0.93 μm^2. There was a substantial variation in size among individual inclusions formed, ranging from 1 μm^2 up to 24 μm^2 in size in different cells. A UV dosage of 250 J/m^2 was chosen for the experiments presented below.

Monitoring of Hirano body formation following promoter induction. To monitor Hirano body formation following promoter induction, five time points were chosen (0, 3, 6, 9, and 24 h), and inclusions formed were measured by direct microscopic observation. Our results demonstrate an increase in the average inclusions size from 0.83 μm^2 before induction to 1.39 μm^2 at 9 hours after promoter induction. However, there was a decrease in the average inclusion area to 1.13 μm^2 at the 24-hour time point. The decrease in Hirano body inclusion size between 9 and 24 h can be attributed to the reduction in the number of cells with Hirano bodies with an area in the 4 to 12 μm^2 range from 10% to 4% within the population. The reduction of inclusions in this midsize range was accompanied by an increase in the number of inclusions in the smallest size category from 82% to 88% and the presence of a few very large inclusions in the 24-h class. These results may also be explained by the events we observed during cell division. During cytokinesis the leading edge of the cells pulls away, forming two daughter cells, and the Hirano bodies get trapped in the cytoplasmic bridge, which can result in the loss of the Hirano body from both cells. These cytoplasmic bridges between daughter cells are the result of cytokinesis B, the typical mode of division for *Dictyostelium discoideum* grown on tissue culture plates. The loss of Hirano bodies during cell division might explain the decrease in size and number of Hirano bodies at 24 h postinduction.

To determine the levels of GFP fluorescence in populations expressing the CT-GFP, flow cytometry was performed. Using this method, we determined that 81% of the population had a GFP signal above background level at 6 hours after promoter induction. At 9 hours, however, the percentage dropped to 70%, and it remained nearly constant at 24 h postinduction (Fig. 3). As a control, cells expressing CT-GFP under the control of the constitutive promoter were evaluated by FACS after UV exposure. We determined that between 86% and 89% of the cells had a GFP signal above background. We did not observe a rise in cells with GFP signal or a rise in fluorescence intensity over time following UV treatment. The experimental data provide a good indication of the average levels of GFP protein within the population. This technique, however, does not provide an indication of the spatial arrangement of the GFP-tagged fusion protein within individual cells.

Observing Hirano body assembly by time-lapse microscopy. It was clear from this and other studies that cells expressing a fragment of the 34-kDa protein (CT) form actin inclusions. To further elucidate the early events during inclusion formation, cells were induced with UV light as described above and incubated in HL-5 medium for 3 h prior to time-lapse recordings. Exposure to the excitation wavelengths necessary for microscopy is toxic to cells over time; therefore, to reduce these effects we used the shortest possible exposure times and the lowest light levels to generate quality images. In the images shown, we can easily determine that small GFP foci develop within the cell; over time these foci fuse to form a single structure (Fig. 4). These inclusions were most often seen at the rear of moving cells.

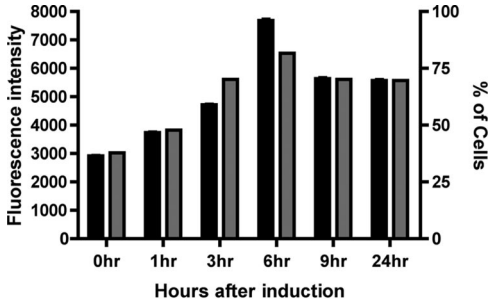

FIG. 3. FACS analysis of the GFP signal intensity in RNR-CT-GFP cells after exposure to UV light. Both the percentage of cells with GFP signal above background (gray bars) and the mean fluorescence intensity of the population (black bars) increases over the first 6 hours after promoter induction. Each bar represents measurement of 10,000 cells at the time point listed on the *x* axis. The error bars represent the standard errors of the means.

DISCUSSION

To date, Hirano bodies have been identified in a number of neurodegenerative diseases, including Pick's disease, amyotrophic lateral sclerosis, and most recently in Alzheimer's disease (7). There is a growing body of evidence that suggests that unregulated protein fragments play a major role in initiating cell toxicity and ultimately cell death (6, 15). Although the underlying mechanisms that lead to protein aggregation and the role in neurodegeneration are still highly debated, the formation of protein aggregates may suggest a possible protective mechanism to prevent cell toxicity. Fusing the CT fragment to GFP under expression of a constitutive and inducible promoter system provided a unique opportunity to observe the formation of actin inclusions in living cells over time.

In this study, we demonstrate that expression of CT fused to a GFP tag does not inhibit the unique ultrastructure previously described for Hirano bodies in the brain or within *Dictyostelium discoideum* (7, 8, 12, 17). From our limited data set, it is not possible to tell whether the presence of the GFP tag causes alterations in the spacing of the filaments within the inclusions observed by TEM; however, large-scale disruptions were not observed.

When cells transformed with the pRNR-CT-GFP vector were exposed to UV light, the percentage of cells with Hirano bodies increased over time. In fact, there was a dose-dependent response between the amount of UV exposure and both the number of cells with Hirano bodies and the size of these inclusions formed within the population. Measuring the size of

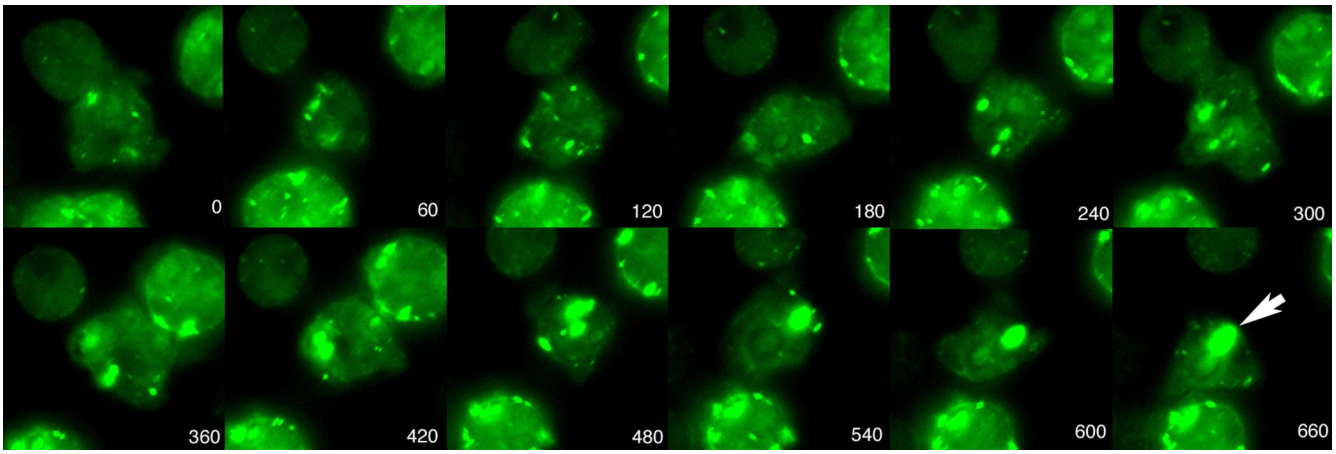

FIG. 4. Time-lapse images of live cells expressing pRNR-CT-GFP. Cells were induced with UV light and incubated for 3 h. A sub-area of a larger image was selected to keep the central cell in the center of the frame. Note the large inclusion (arrow) that forms in the central cell as smaller inclusions merge. Time is represented in seconds after the beginning of image collection.

Hirano bodies in individual cells, we further determined that the maximal size and number of Hirano bodies formed within 9 hours after promoter induction. FACS analysis provided a better indication of GFP expression levels across the whole population over time. We observed an increase in the mean fluorescence intensity in the first hour postinduction, with a peak in the mean fluorescence of the population at 6 hours. The levels of fluorescence stabilized after 9 hours and remained constant throughout the population at 24 h postinduction. These results are consistent, given the expression profile of the RNR promoter system.

These observations also correlate with our findings that Hirano bodies are formed by aggregation of many small inclusions. At 9 hours the mean fluorescence intensity observed by FACS has dropped, but the average size of the Hirano bodies observed by microscopy increased. After 24 h, our microscopic observations indicate that the number of cells with inclusions in the middle of our observed size range is substantially reduced, with a relatively small group of cells retaining large aggregates and the majority of the population maintaining small aggregates, a characteristic of basal level expression. These observations fit with the hypothesis that cells assemble the aggregated actin fragments into large inclusions and that these inclusions may be lost during cell division.

The use of an inducible promoter system allowed us to observe the fate of the GFP-labeled molecules over time. In most instances, the GFP aggregates fused into a single aggregate prominently visible at the back of the cell. These observations are consistent with the work of Lee et al. (9), who observed patches of actin bound with labeled phalloidin aggregating at the rear of the cell after introduction of phalloidin into cells by electroporation. These results are consistent with the mechanism suggested by Davis et al. (1), based on their observations of static images. The ability to initiate Hirano body formation in living cells and observe the early morphological events during protein aggregate formation might now allow us to characterize the mechanisms or regulatory proteins that drive or inhibit the formation of these inclusions in living cells. Furthermore, our model system might provide additional information regarding the toxicity or protective mechanisms associated with protein inclusion formation in living cells and further elucidate the mechanism associated with protein inclusion formation in neurodegenerative diseases.

ACKNOWLEDGMENTS

We thank Ramon Castro and the Chicago State University Core Microscopy Facility for help with both electron and light microscopy. The FACS analysis was completed at the Chicago State University Flow Cytometry Facility with the help of Abdelrahman Elarja and Ashraf Ali. We also thank Denise Patrick for help with cell line maintenance and general lab support. The *Dictyostelium* Stock Center provided base vectors and wild-type cell lines (http://dictybase.org/).

The project described was supported by grant S06 GM008043 from the National Institute of General Medical Sciences. Additional support from the NIH-funded Chicago State University-Northwestern University Bridge to the Ph.D. program was provided to J. F. Reyes and J. Ramos. Funds to establish the FACS facility were provided by NSF/MRI 0520869.

REFERENCES

1. **Davis, R. C., R. Furukawa, and M. Fechheimer.** 2008. A cell culture model for investigation of Hirano bodies. Acta Neuropathol. **115:**205–217.
2. **Fey, P., A. S. Kowal, P. Gaudet, K. E. Pilcher, and R. L. Chisholm.** 2007. Protocols for growth and development of *Dictyostelium discoideum.* Nat. Protoc. **2:**1307–1316.
3. **Galloway, P. G., G. Perry, and P. Gambetti.** 1987. Hirano body filaments contain actin and actin-associated proteins. J. Neuropathol. Exp. Neurol. **46:**185–199.
4. **Gaudet, P., H. MacWilliams, and A. Tsang.** 2001. Inducible expression of exogenous genes in *Dictyostelium discoideum* using the ribonucleotide reductase promoter. Nucleic Acids Res. **29:**E5.
5. **Gaudet, P., K. E. Pilcher, P. Fey, and R. L. Chisholm.** 2007. Transformation of *Dictyostelium discoideum* with plasmid DNA. Nat. Protoc. **2:**1317–1324.
6. **Hardy, J., and D. J. Selkoe.** 2002. The amyloid hypothesis of Alzheimer's disease: progress and problems on the road to therapeutics. Science **297:** 353–356.
7. **Hirano, A.** 1994. Hirano bodies and related neuronal inclusions. Neuropathol. Appl. Neurobiol **20:**3–11.
8. **Hirano, A., H. M. Dembitzer, L. T. Kurland, and H. M. Zimmerman.** 1968. The fine structure of some intraganglionic alterations. Neurofibrillary tangles, granulovacuolar bodies and "rod-like" structures as seen in Guam amyotrophic lateral sclerosis and parkinsonism-dementia complex. J. Neuropathol. Exp. Neurol. **27:**167–182.
9. **Lee, E., E. A. Shelden, and D. A. Knecht.** 1998. Formation of F-actin aggregates in cells treated with actin stabilizing drugs. Cell Motil. Cytoskeleton **39:**122–133.

10. **Levi, S., M. Polyakov, and T. T. Egelhoff.** 2000. Green fluorescent protein and epitope tag fusion vectors for *Dictyostelium discoideum.* Plasmid **44:**231–238.
11. **Manstein, D. J., H. P. Schuster, P. Morandini, and D. M. Hunt.** 1995. Cloning vectors for the production of proteins in *Dictyostelium discoideum.* Gene **162:**129–134.
12. **Maselli, A., R. Furukawa, S. A. Thomson, R. C. Davis, and M. Fechheimer.** 2003. Formation of Hirano bodies induced by expression of an actin cross-linking protein with a gain-of-function mutation. Eukaryot. Cell **2:**778–787.
13. **Maselli, A. G., R. Davis, R. Furukawa, and M. Fechheimer.** 2002. Formation of Hirano bodies in *Dictyostelium* and mammalian cells induced by expression of a modified form of an actin-crosslinking protein. J. Cell Sci. **115:** 1939–1949.
14. **Novak, K. D., M. D. Peterson, M. C. Reedy, and M. A. Titus.** 1995. *Dictyostelium* myosin I double mutants exhibit conditional defects in pinocytosis. J. Cell Biol. **131:**1205–1221.
15. **Rankin, C. R., and T. C. Gamblin.** 2008. Assessing the toxicity of Tau aggregation. J. Alzheimers Dis. **14:**411–416.
16. **Sambrook, J., and D. Russel.** 2001. Molecular cloning: a laboratory manual, 3rd ed. Cold Spring Harbor Labortory Press, Cold Spring Harbor, NY.
17. **Schochet, S. S., Jr., and W. F. McCormick.** 1972. Ultrastructure of Hirano bodies. Acta Neuropathol. **21:**50–60.